

Anion- and Solvent-Induced Rotary Dynamics and Sensing in a Perylene Diimide [3]Catenane

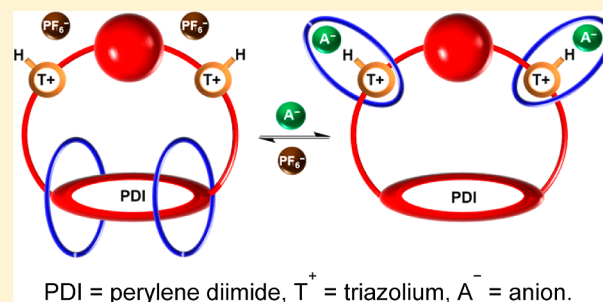
Timothy A. Barendt,[†] Liliana Ferreira,^{‡,§} Igor Marques,^{‡,§} Vítor Félix,^{‡,§} and Paul D. Beer^{*,†,§}

[†]Chemistry Research Laboratory, Department of Chemistry, University of Oxford, 12 Mansfield Road, Oxford OX1 3TA, United Kingdom

[‡]Department of Chemistry, CICECO–Aveiro Institute of Materials, and [§]Department of Medical Sciences, iBiMED–Institute of Biomedicine, University of Aveiro, 3810-193 Aveiro, Portugal

S Supporting Information

ABSTRACT: A novel dynamic [3]catenane consisting of a large four-station central macrocycle which incorporates a bay tetrachloro-functionalized perylene diimide (PDI) unit and two triazolium anion-binding motifs, mechanically bonded with two smaller isophthalamide-containing macrocycles, is constructed using an anion template synthetic methodology. Proton NMR, electronic absorption, and fluorescence emission spectroscopies together with molecular dynamics simulations are used to investigate the anion recognition- and solvent-dependent dynamic properties of the higher-order mechanically interlocked molecule. Importantly, unprecedented solvent-dependent and anion-binding-induced circumrotatory motion in a hetero[3]catenane system is demonstrated where the exotic dual rotary switching behavior provides a unique and sophisticated mechanism for optical anion sensing in competitive protic organic and aqueous–organic media.



INTRODUCTION

In the 26 years since the first rotaxane-based molecular shuttle was reported,¹ mechanically interlocked molecules (MIMs) have become firmly established within the field of nanoscale molecular machines and switches.^{2–4} The ability to undergo controlled and reversible molecular motion via changes in the relative positions of their constituent parts, as dictated by the nature of the inherent mechanical bond, has been key to this success.^{5–10} Furthermore, MIMs containing more than two interlocked components may be used to promote motions of even greater complexity that, for example, mimic the actions of an elevator,¹¹ compressor,^{12,13} or pincer^{14–17} from the macroscopic world.

While a variety of light,^{18,19} redox,^{20,21} and chemical^{22–25} stimuli have been utilized to promote and control co-conformational change in MIMs, exploiting their unique topological host cavities and dynamic properties for guest-induced shuttling or co-conformational switching as a sophisticated means of achieving molecular guest recognition and sensing, however, remains underdeveloped. Currently the number of reported examples of metal cation guest-driven switches^{2,26–28} far outweighs anion-based analogues,^{15,29–45} which is perhaps surprising given the fundamental roles negatively charged species play in a range of chemical, biological, and environmental processes.⁴⁶

Within the category of anion-mediated molecular switches, translational motion has been demonstrated in a number of multi-station rotaxanes,^{15,29–43} including a recent example of a

[3]rotaxane that produces pincer-like motion of its two macrocycle components upon oxoanion binding.¹⁵ However, examples of anion controlled rotations of interlocked rings in catenanes are considerably rarer.^{47–49} To date, discrete anion recognition has served as a stimulus for rotary motion in a homocatenane⁵⁰ whereas, to the best of our knowledge, the challenging circumrotation of one macrocycle around another in a heterocatenane⁵¹ (akin to rotaxane shuttling) stimulated by anion binding has yet to be realized.⁵³ Furthermore, anion-binding-induced elaborate rotational motions in higher-order catenanes is unprecedented.

Providing a readily functionalizable electron-deficient scaffold with excellent chromophoric, emissive, and redox properties, perylene diimide (PDI) derivatives have become increasingly prevalent in the construction of supramolecular materials.^{54–56} Their growth has also been fuelled by the ability of PDI compounds to participate in a variety of non-covalent interactions, with self-aggregation via intermolecular aromatic stacking being the most commonly exploited.^{57–59} While this has been imaginatively utilized to direct supramolecular self-assembly,^{55,60} the isolation of individual molecular species in solution is critical to the pursuit of controlling the dynamics of a mechanically interlocked system (*vide supra*). This may explain why only a handful of MIMs containing PDI derivatives have been isolated.^{61–65} One approach to inhibit the formation

Received: May 4, 2017

Published: June 7, 2017

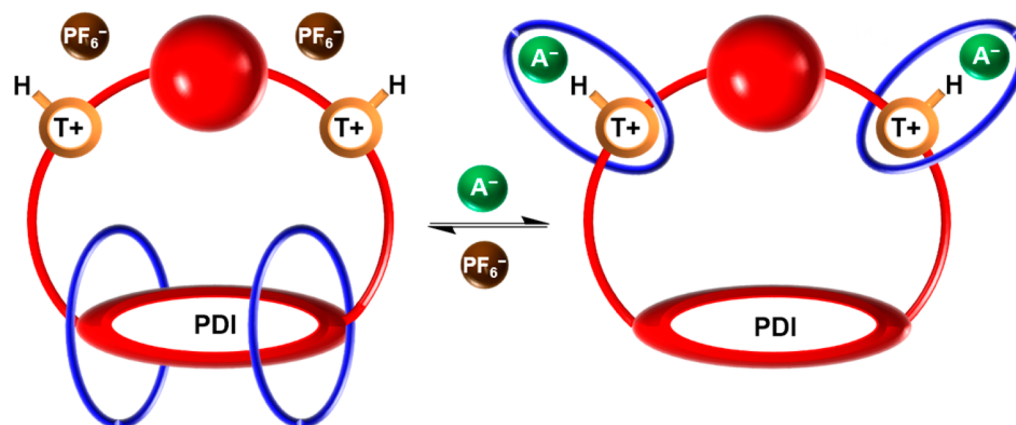


Figure 1. Schematic of the anion-induced circumrotatory molecular motion exhibited by a four-station PDI-bis-triazolium hetero[3]catenane. PDI = tetrachloro perylene diimide, T⁺ = triazolium, A[−] = anion.

of aggregates is via the introduction of substituents in the PDI bay (1,6,7,12) positions where sterics impart a propeller-type contortion of the aromatic framework away from planarity.⁶⁶ In addition to improving solubility and electron deficiency, we envisaged that the two naphthalimide subunits formed by the core tetrachlorination^{67,68} of PDI would act as dual recognition sites allowing this motif to accommodate two hydroquinone-based macrocycles courtesy of aromatic donor–acceptor π -stacking between electron-rich and electron-deficient aromatic rings.

Herein we report the synthesis of a novel dynamic [3]catenane consisting of a large four-station central macrocycle which incorporates a tetrachloro-functionalized PDI unit and two triazolium anion-binding motifs, and two smaller macrocycles containing isophthalamide anion-binding sites. This heterocatenane is demonstrated to undergo large-amplitude circumrotational anion recognition-induced molecular motion through the positional bias of the two peripheral macrocycles (Figure 1). Importantly, we also demonstrate that this exotic dual rotary switching behavior can be exploited as a novel mechanism for optical anion sensing in protic organic and aqueous–organic media.

RESULTS AND DISCUSSION

Synthesis of the Hetero[3]catenane. The [3]catenane was prepared by a multi-step synthetic pathway as fully detailed in the [Supporting Information \(SI\)](#). Initially, a [1+1] macrocyclization reaction was performed in which a tetrachloro-PDI bis-biphenyl azide derivative was ring closed with a phenyl trityl bis-alkyne via a double copper(I)-catalyzed azide alkyne cycloaddition (CuAAC) “click” reaction under high dilution conditions to afford the large, rigid central ring (Scheme 1). Subsequent methylation of the triazole heterocycles and anion exchange to the chloride salt afforded the desired dicationic cyclic species **1**·(Cl)₂ in an overall yield of 40%.⁶⁹

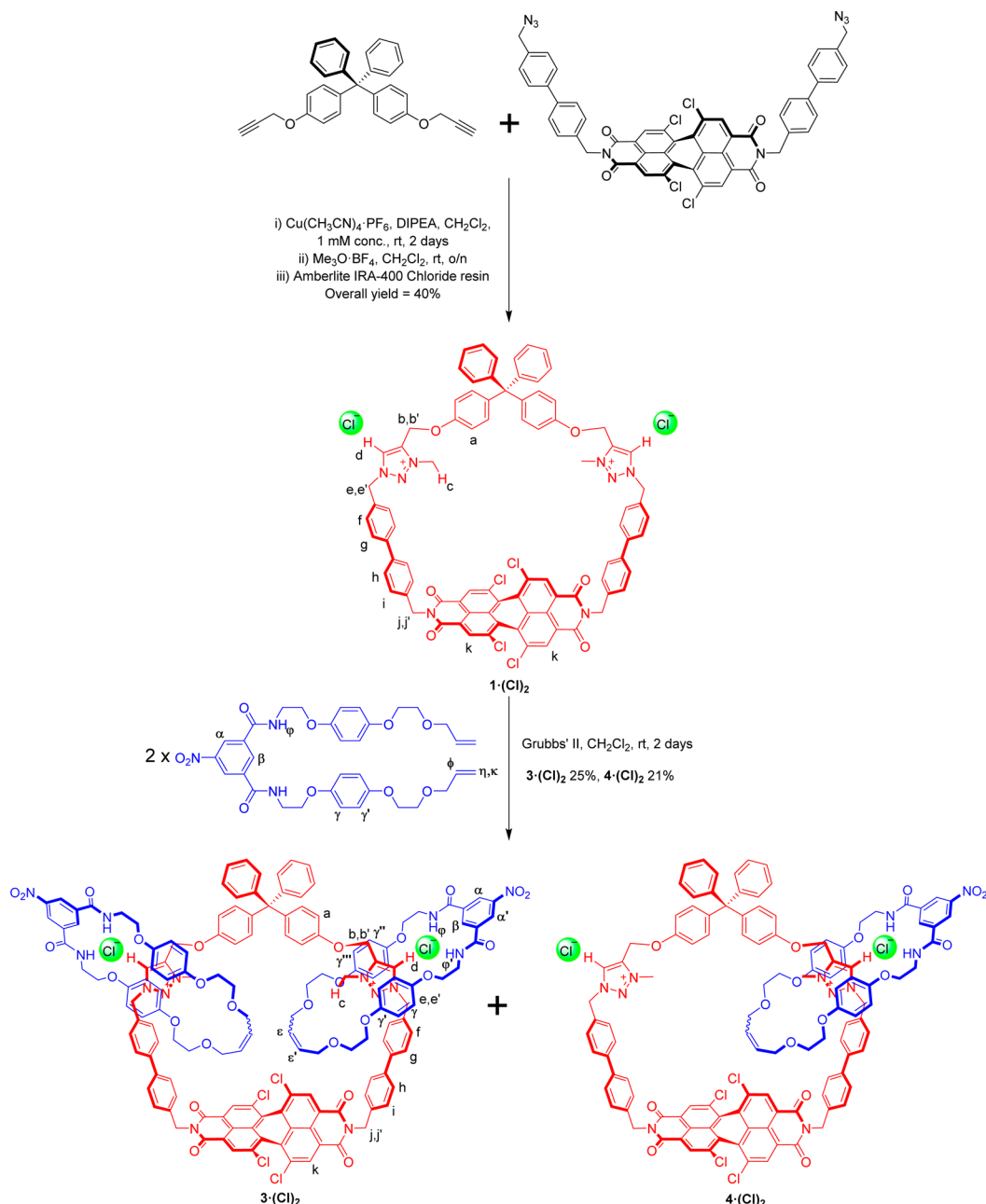
For catenane formation, chloride anion templation was used to facilitate the ring closing metathesis of two bis-vinyl-functionalized 5-nitro-isophthalamide macrocycle precursors **2** around the central four-station bis-triazolium tetrachloro PDI macrocyclic wheel **1**·(Cl)₂ using Grubbs’ II catalyst in dry dichloromethane (Scheme 1). Preparative silica thin-layer chromatography purification led to the isolation of the target [3]catenane **3**·(Cl)₂ in 25% yield together with the [2]catenane **4**·(Cl)₂ byproduct, in a yield of 21%. Both catenanes were

characterized by ¹H, ¹³C, and two-dimensional ¹H ROESY NMR spectroscopy and high-resolution mass spectrometry (see SI, section 2).⁷¹

¹H NMR Rotary Motion Investigations. In order to assess the dynamic nature of [3]catenane **3**·(A)₂ one- and two-dimensional ¹H NMR spectroscopy was used to identify the predominant co-conformations of the coordinating (A = Cl[−]) and non-coordinating (A = PF₆[−]) anion salts in CDCl₃ (Figure 2).

In the case of **3**·(Cl)₂ the coordination of two chloride anions between the orthogonal cyclic components by hydrogen bonding results in the peripheral isophthalamide-containing macrocycles residing at the triazolium stations of the large central macrocycle. This co-conformation is supported by a ¹H–¹H ROESY NMR spectrum (Figure S1) and the fact that formation of the [3]catenane induces no perturbation of the PDI protons H_k but instead reveals diastereotopic splitting of the central macrocycle’s methylene protons on either side of the triazolium stations, H_{b/b′} and H_{e/e′} (Figure 2a). The observation that the atropisomerism of the PDI unit is propagated to this region of the central macrocycle is indicative of significant rigidity and steric constraint in this co-conformation. As a consequence, a degree of restricted pirouetting of the peripheral macrocycles around the triazolium groups is also observed; their desymmetrization produces a set of resonances for each of the external isophthalamide aromatic protons (H_α and H_{α′}) and for each hydroquinone aromatic ring (H_{γ,γ′} and H_{γ′,γ″}).⁷³ The adoption of separate (asymmetric) co-conformations by each isophthalamide macrocycle can be ruled out because comparison of the ¹H NMR spectra of [3]- and [2]catenanes, **3**·(Cl)₂ and **4**·(Cl)₂, respectively, reveals identical desymmetrization in both, even at low temperature (Figure S2a). Therefore, the same through-space interaction patterns are also seen in the two-dimensional ¹H ROESY NMR spectrum of the [2]catenane (Figure S3). However, in contrast to the [3]catenane, the presence of separate singlet resonances for proto-triazolium protons H_b and H_{b′} in the [2]catenane reveals that the isophthalamide macrocycle cannot pass over either the phenyl trityl spacer unit or the tetrachloro PDI motif, and so the position of each smaller ring is sterically restricted to one half of the larger central ring (Figure S2b).

Comparison of the ¹H NMR spectra of **3**·(Cl)₂ and **3**·(PF₆)₂ in CDCl₃ revealed, surprisingly, that anion exchange to the bis-hexafluorophosphate salt resulted in no shift in the PDI protons H_k and only small perturbations to protons along the track of

Scheme 1. Chloride-Templated Syntheses of Hetero[3]- and -[2]catenanes $3\cdot(\text{Cl})_2$ and $4\cdot(\text{Cl})_2$ 

the central ring ($\text{H}_{\text{e,b,j}}$), indicating negligible circumrotational motion (Figure 2). In $3\cdot(\text{PF}_6)_2$ the sustained occupancy of the triazolium stations may be explained by favorable hydrogen bonding interactions between the polyether cavities of the two peripheral macrocycles and the polarized *N*-methyl triazolium protons, an effect that is manifested in the downfield shift of H_{c} (Figure 2). Interestingly the subtle co-conformational changes that occur to accommodate these non-covalent interactions cause the isophthalamide aromatic protons H_{α} and $\text{H}_{\alpha'}$ to become equivalent suggesting there is now more flexibility in the positions of the smaller rings. Therefore, in CDCl_3 , the removal of the coordinating halide anions from the [3]catenane “unlocks” the peripheral macrocycles affording them a greater degree of pirouetting motion (Figure 2). Interestingly, interchange between all the triazolium-based co-conformers occurs on a time scale faster than that of the NMR experiment

which, despite the desymmetrization of the peripheral macrocycles, produces relatively simplistic NMR spectra (*vide infra*).

Taking into account the solvent dependency of non-covalent aromatic stacking interactions,^{74–85} and in particular on the formation of self-aggregated PDI π -stacks,^{57,86,87} an investigation into the effect of increasing the polarity of the solvent medium on the predominant co-conformation of the [3]-catenane salts was undertaken.

With the assistance of two-dimensional HSQC NMR, a comparison of the ^1H NMR spectrum of $3\cdot(\text{PF}_6)_2$ in CDCl_3 and 3:1 CDCl_3 : CD_3OD suggests that the polar protic solvent mixture causes the [3]catenane to adopt a new co-conformation that arises from circumrotatory motion of the peripheral macrocyclic wheels to the two naphthalimide subunits of the twisted PDI scaffold (Figure 3a,b). Specifically, the addition of CD_3OD was found to increase the complexity of

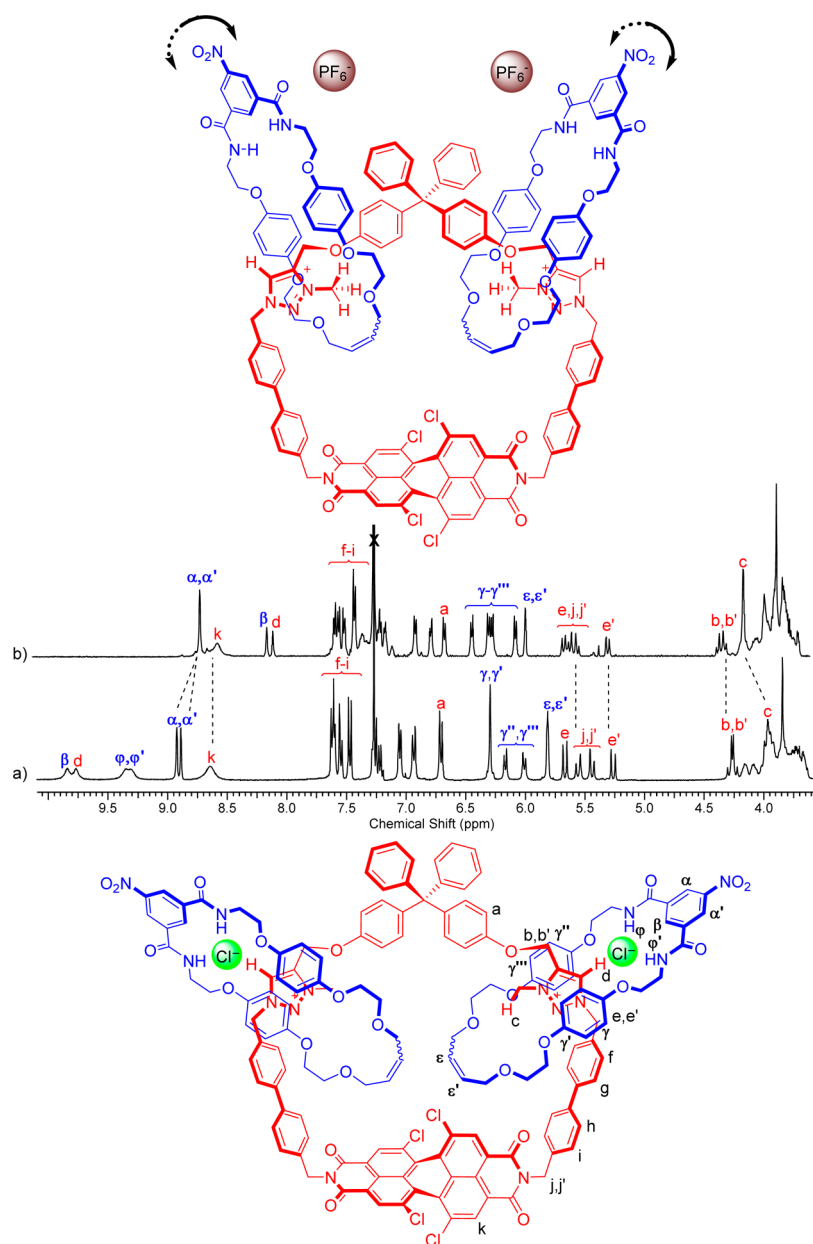


Figure 2. Truncated ^1H NMR spectra of (a) bis-chloride and (b) bis-hexafluorophosphate salts of [3]catenane $3\cdot(\text{A})_2$ (CDCl_3 , 298 K, 400 MHz) and the co-conformations associated with each. Black arrows indicate the greater potential for pirouetting rotary motion of the peripheral macrocycles around the triazolium stations in $3\cdot(\text{PF}_6)_2$. All the tetrachloro PDI compounds reported in this work were isolated as a racemic mixture of two atropisomers that exist as a result of the twisted PDI scaffold.⁶⁹

the ^1H NMR spectrum, to a degree that cannot be accounted for by further desymmetrization of the peripheral rings (Figures 3a and S4).⁸⁸ Instead, the appearance of chemical exchange peaks in the ^1H – ^1H ROESY NMR spectrum (Figure S7) implies highly restricted isophthalamide macrocycle pirouetting in the new PDI-based co-conformation and hence the effects of slow exchange on the NMR time scale (Figure 3a). Taking into account that the peripheral macrocycles cannot pass over the bulky PDI motif because of the chlorine substituents in the bay positions it is perhaps not surprising that the new aromatic stacking interactions between the interlocked components are susceptible to a significant degree of steric constraint. Indeed, complex NMR signal patterns have also been reported for PDI derivatives in which bulky substituents produce restricted rotation about the C–N bond at the imide termini.^{89–91}

Importantly the ^1H – ^1H ROESY NMR spectrum also revealed new through-space proton couplings that were indicative of intramolecular facial aromatic stacking interactions between the electron-rich hydroquinone groups of the peripheral macrocycles and the electron-deficient tetrachloro PDI motif that further support the nature of this co-conformational change (Figure S8). While solvophobic effects are thought to provide the thermodynamic driving force for this, occupancy of the PDI stations in $3\cdot(\text{PF}_6)_2$ is also enhanced upon the introduction of water (i.e., in 45:45:10 CDCl_3 : CD_3OD : D_2O) because of a hydrophobic contribution⁵⁷ toward the aromatic stacking interactions (Figures S4 and S9).

In summary, the significant high- or low-field shifting of signals and overall complex pattern of the spectrum of $3\cdot(\text{PF}_6)_2$ in 3:1 CDCl_3 : CD_3OD can be interpreted in terms of shielding

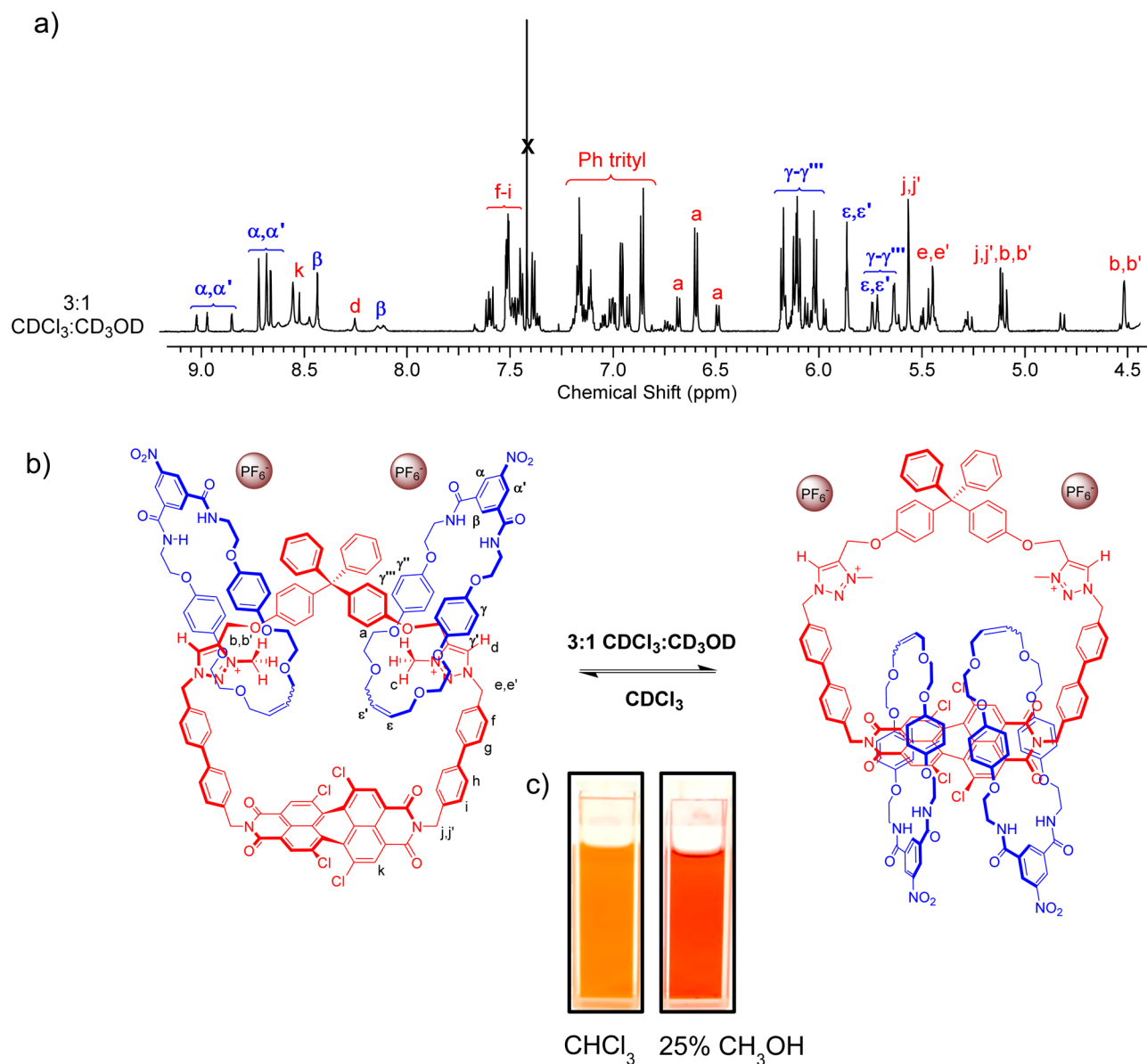


Figure 3. Solvent-induced circumrotatory motion. (a) Truncated ^1H NMR spectrum of the bis-hexafluorophosphate salt of [3]catenane $3\cdot(\text{PF}_6)_2$ in 3:1 $\text{CDCl}_3:\text{CD}_3\text{OD}$ (CDCl_3 , 298 K, 400 MHz). (b) The co-conformations and (c) the colors associated with each solvent.

or deshielding of protons by the interacting π systems of the three interlocked macrocyclic rings and the existence of slowly exchanging PDI-based co-conformers of the [3]catenane under these solvent conditions.

The addition of further aliquots of CD_3OD had the effect of further increasing the complexity of the ^1H NMR spectrum suggesting that the increasing solvent polarity acts to favor the hydroquinone-containing macrocycle's affinity for the PDI stations (Figure S4). Poor solubility of $3\cdot(\text{PF}_6)_2$ and a significant degree of signal broadening at higher percentages of CD_3OD negated further one- and two-dimensional ^1H NMR investigation.

Chemical exchange peaks and through-space proton couplings in the ^1H – ^1H ROESY NMR spectrum revealed that the peripheral macrocycles of $3\cdot(\text{PF}_6)_2$ also resided at the PDI stations when the solvent system was switched to d_6 -DMSO (Figure S10), enabling variable temperature (VT) ^1H NMR spectroscopy to be performed up to 130 °C (Figure S11). Significant broadening and coalescence of peaks,

indicative of an intermediate regime, only began to occur at 100 °C, which reveals that the energetic barrier to permit free pirouetting of the macrocycles at the PDI stations, and thus more-rapid exchange between PDI-based co-conformers, is relatively high.

While the ^1H NMR spectrum of the [3]catenane bis-chloride salt $3\cdot(\text{Cl})_2$ in 3:1 $\text{CDCl}_3:\text{CD}_3\text{OD}$ also exhibits the effects of slow-exchange⁹² (*vide supra*), comparison with the bis-hexafluorophosphate analogue revealed an overall downfield shift of the hydroquinone proton resonances ($H_{\gamma-\gamma''}$) and signals associated with the aromatic PDI protons (H_k) (Figure S12). This is indicative of peripheral macrocycle occupancy of the anion-binding triazolium stations (i.e., halide anion-induced circumrotatory motion), which is also evidenced by new through-space interactions in the two-dimensional ^1H ROESY NMR spectrum of $3\cdot(\text{Cl})_2$ (Figure S13).

Molecular Modeling. Further insights into the [3]catenane anion-induced rotary motions were obtained at the atomistic level through molecular dynamics (MD) simulations under-

taken within the AMBER16 software package.⁹³ The [3]-catenane's components were described with General Amber Force Field (GAFF) parameters^{94,95} and using Restricted Electrostatic Potential (RESP) charges.⁹⁶ The remaining classical force field parameters and simulation details are given in the SI.

A preliminary conformational analysis carried out in the gas phase by quenched MD run on the free larger PDI macrocycle **1** yielded a representative structure with a well-defined circular shape, as shown in Figure S14. On the other hand, the structure of the peripheral macrocycles was taken directly from the macrocycle single-crystal X-ray structure deposited with the Cambridge Structural Database⁹⁷ (see SI for details), with the alkene fragment on the ether loop adopting a *trans* configuration. Two isophthalamide macrocycles and a PDI station were assembled, yielding the [3]catenane. The isophthalamide clefts from the peripheral macrocycles and the triazolium stations' C–H_d are interlocked in an orthogonal binding arrangement, affording co-conformation **3_A**, with the isophthalamide clefts in opposite positions relative to the plane defined by the framework of the PDI macrocycle. This starting co-conformation was further used to investigate the pirouetting and circumrotatory motions of the [3]catenane in the presence of either two coordinating (Cl[−]) or non-coordinating (PF₆[−]) anions.

The starting conformation with a chloride anion lodged in each binding pocket, **3_A·(Cl)₂** (Figure 4), was immersed in

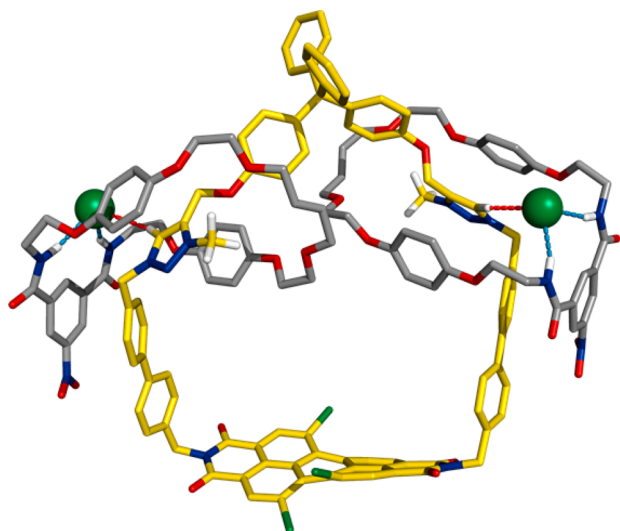


Figure 4. Molecular mechanics structure of co-conformation **3_A·(Cl)₂**, with the N–H_ψ···Cl[−] and C–H_d···Cl[−] hydrogen bonds drawn as blue or red dashed lines. The carbon atoms of the peripheral and central PDI macrocycles are colored in gray and yellow, respectively, while the remaining atoms are colored with the standard CPK rules. The chloride anions are drawn in spheres. Most of the C–H hydrogen atoms have been omitted for clarity.

cubic boxes composed of 1219 chloroform and 803 methanol molecules, randomly distributed, in agreement with a 3:1 (v/v) CHCl₃:CH₃OH solvent mixture as used in the ¹H NMR studies. Two independent replicates were carried out under periodic boundary conditions following a multi-stage protocol (see SI, section 4.4) and using the PMEMD executable with GPU acceleration as simulation engine.⁹⁸

The dynamic behavior of **3_A·(Cl)₂** was ascertained throughout the 100 ns of sampling time, monitoring the

distances from the chloride anions to the carbon atoms of triazolium stations (C–H_c···Cl[−] and C–H_d···Cl[−]). The evolution of these distances is plotted along the counting of the N–H_ψ···Cl[−] hydrogen bonding interactions in Figure S15 for both MD replicates, and the dimensions of the hydrogen bonds to the isophthalamide macrocycles are summarized in Table S1.

Overall, throughout most of the MD simulation time, each chloride anion maintains two N–H_ψ···Cl[−] hydrogen bonds with the isophthalamide clefts of the peripheral macrocycles, and these are assisted by C–H_{c/d}···Cl[−] bonds with the triazolium station protons. Strikingly, the interruption of the N–H_ψ···Cl[−] hydrogen bonds monitored along the two independent MD runs is intermittent and unrelated with significant co-conformational changes on the [3]catenane. This provides a clear indication that, in agreement with ¹H NMR spectroscopy studies (*vide supra*), the isophthalamide macrocycles can reside at the triazolium stations in the 3:1 (v/v) CHCl₃:CH₃OH solvent mixture due to convergent hydrogen bonding interactions from the interlocked components toward the chloride guest. On the other hand, the evolution of the triazolium C–H_{c/d}···Cl[−] distances plotted in Figure S15 shows that at ca. 15 ns of the first MD replicate, one of the C–H_d···Cl[−] interactions is replaced by C–H_c···Cl[−] ones, while the N–H_ψ···Cl[−] hydrogen bonds are preserved. In other words, the triazolium unit of the central ring has rotated within its peripheral macrocycle, as illustrated in Figure S16 and further discussed in section 4.2 of the SI.

In addition, there is pirouetting motion of the peripheral isophthalamide macrocycles around the triazolium stations. This structural feature is clearly shown in Figure S17 (left), with the 3D surface histogram built with the positions occupied along the second MD run by the centers of mass defined by the two nitrogen atoms of each isophthalamide cleft (equivalent results were observed for the first MD replicate). While one of the peripheral macrocycles is able to pirouette around its triazolium station (blue cloud), the rotation of the other ring (red cloud) is more restricted and undergoes only half a pirouetting motion. On the other hand, these histograms also indicate that the most common positions (the larger regions of the clouds) of the binding clefts result from a more restricted motion.

To ascertain the influence of solvent polarity on pirouetting motions, **3_A·(Cl)₂** was also investigated in pure chloroform through two independent MD runs of 100 ns each (see SI, section 4.4). In both replicates, the two chloride anions are maintained tightly bonded to the isophthalamide clefts by two convergent N–H_ψ···Cl[−] hydrogen bonds together (see Table S2)⁹⁹ with C–H_d···Cl[−] hydrogen bonds (Figure S18). Hence, the pirouetting motions observed for both peripheral macrocycles are limited to only a half turn (see Figure S19), which is in agreement with observations from the previous ¹H NMR spectroscopic studies in CDCl₃. Furthermore, the MD results obtained in both solvent media also support the theory (*vide supra*) that desymmetrization of the macrocyclic rings occupying the triazolium stations is, in part, responsible for the complex ¹H NMR spectra obtained in solution.

Following the ¹H NMR spectroscopic findings in the 3:1 (v/v) CDCl₃:CD₃OD solvent mixture, the ability of the peripheral macrocycles to interact with the PDI station in the presence of chloride anions was also evaluated. Thus, both isophthalamide macrocycles hydrogen bonded to the chloride anions were relocated to the tetrachloro perylene diimide motif, affording

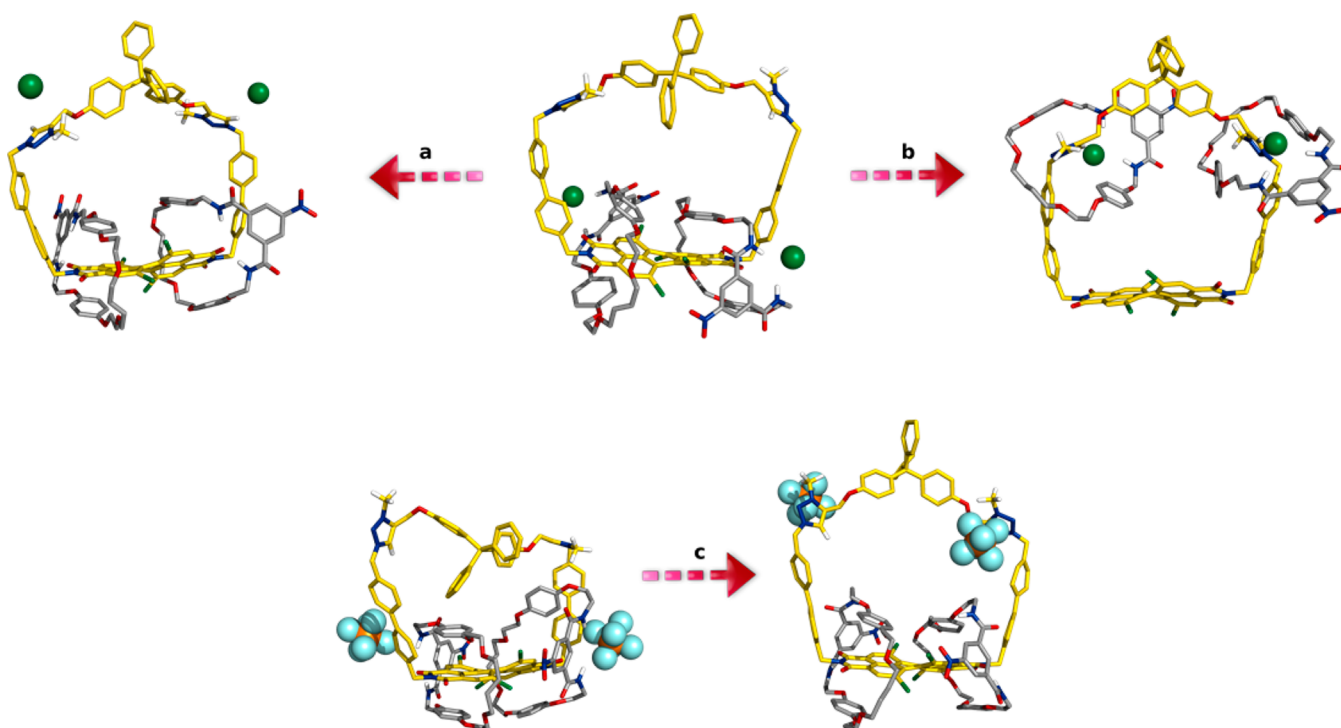


Figure 5. Co-conformation changes of **3** in the presence of two coordinating chloride (top) or two hexafluorophosphate (bottom) anions. The conformational change (path a) was observed in MD simulations without distance restraints between the isophthalamide N–H_ψ groups and the chloride anions. The co-conformational change (path b) was observed when N···Cl[−] distances were restrained in 3:1 CHCl₃:CH₃OH (anion stimulus) or without any restraints in CHCl₃ (solvent stimulus). The change between scenarios shown in path c was observed in the solvent mixture. Coloring details as given in Figure 4.

the starting conformation **3_B**·(Cl)₂ with the two electron-rich hydroquinones from each peripheral macrocycle establishing facial aromatic stacking interactions with a side of the extended electron-deficient PDI moiety. Two independent MD runs with sampling periods of 100 ns each with these new binding arrangements were performed using the same multi-stage simulation protocol for **3_A**·(Cl)₂. Both chloride anions migrate toward the positively charged triazolium stations during the equilibration stage, while the peripheral macrocycles remain at the PDI station until the end of simulation, as shown in Figure 5 (co-conformation change path a). Indeed, in both replicates, the aromatic stacking interactions between the PDI station and the hydroquinone rings are preserved throughout most of the simulation time with inter-aromatic distances C_{HYD}···C_{PDI} of 3.730 ± 0.410 Å (Table S3).¹⁰⁰ Furthermore, these are assisted by intermittent N–H_ψ···O hydrogen bonds to the imide carbonyl groups, which are sporadically replaced by N–H_ψ···Cl ones with the PDI chlorine substituents (Table S4). These cooperative non-covalent interactions significantly restrict pirouetting of the isophthalamide macrocycles at the PDI stations (to a far greater degree than at the triazolium stations) and so, alongside structural rigidity and steric restraint, are the likely cause of the slow rotations of the interlocked rings that induce significant complexity from chemical exchange in the ¹H NMR spectra (*vide supra*). This structural feature is precisely illustrated in Figure S17 (right).

Given that the simulations reported above show that the anions were electrostatically attracted to the triazolium stations, the following question arises: does the coordination of chloride anions by the peripheral isophthalamide macrocycles trigger their circumrotatory motion to the triazolium stations as suggested by the ¹H NMR studies? Thus, the previous

simulations were repeated with weak harmonic restraints on the N···Cl[−] distances (i.e., mimicking the anion stimulus), since the hydrogen bonding interactions in GAFF^{94,95} are accounted in the electrostatic and van der Waals interactions. With the application of these distance restraints, we observed the restricted circumrotation of both macrocycles hydrogen bonded to their anions from the PDI stations to the triazolium ones, thus converting **3_B**·(Cl)₂ into **3_A**·(Cl)₂, as clearly depicted in Movie S1 and Figure 5 (path b).

As suggested by the ¹H NMR data, the hetero[3]catenane's circumrotatory motion is induced by changing the nature of the anion. To demonstrate this, the interactions between hexafluorophosphate anions and **3** were investigated in the solvent mixture, starting with **3_B**·(PF₆)₂, in which the polyatomic anions were positioned near the isophthalamide binding units of the peripheral macrocycles and at the PDI station. Analogous to the MD simulations with **3_B**·(Cl)₂ without restraints, the PF₆[−] anions freely migrate to the triazolium stations within the first nanoseconds of simulation time, while the peripheral macrocycles are held to the PDI station by aromatic stacking and hydrogen-bonding interactions to the PDI station, as described above (Figure 5, path c).

For comparison purposes, the dynamic behavior of **3_B**·(Cl)₂ was also investigated by MD simulation for 100 ns immersed in a pure chloroform solvent box. Noteworthy, in the absence of competitive methanol molecules, both chloride anions, tightly bonded to the isophthalamide macrocycles, independently migrate toward the triazolium stations within the first 2 ns of MD simulation, akin to the simulations in the chloroform–methanol solvent mixture and in agreement with the corresponding ¹H NMR spectroscopic characterization of solvent-induced molecular motion. In other words, the use of

$N\cdots Cl^-$ distance restraints in the competitive solvent mixture (i.e., an anion stimulus) or the removal of the competitive methanol molecules (i.e., a solvent stimulus) leads to the large-amplitude circumrotatory motion of the peripheral macrocycles (Figure 5, path b). In this context, it is important to note that the chloride anions are more extensively solvated by methanol molecules rather than by chloroform ones, as further discussed in the SI, section 4.2.

In summary, these MD simulations demonstrate there is some, albeit relatively restricted, pirouetting motion of the peripheral macrocyclic rings in the triazolium-based co-conformers of the [3]catenane in solution, while in the PDI-based analogues there is significant restraint, which serves to explain the complex 1H NMR spectra obtained upon the addition of polar protic solvent. Importantly, with the simulations carried out on the starting co-conformation $3_B \cdot (Cl)_2$, when $N-H\cdots Cl^-$ distances restraints were applied in the methanol–chloroform solvent mixture, chloride anion-binding-induced circumrotatory molecular motion of the peripheral macrocycles from the PDI stations to the triazolium anion recognition sites takes place. Furthermore, the stimulus of solvent exchange to pure chloroform had the same effect.

Optical UV–Visible and Fluorescence Solvent-Dependent Rotary Motion Studies. The solvent-dependent induced circumrotatory motion of $3 \cdot (PF_6)_2$ also elicited a distinct naked-eye color change of the solution from orange in $CDCl_3$ to red in 3:1 $CDCl_3:CD_3OD$ (Figure 3c). Further investigation of the [3]catenane's dynamic behavior was therefore undertaken using UV–vis spectroscopy to monitor the electronic spectrum of $3 \cdot (PF_6)_2$ in increasingly polar $CHCl_3:CH_3OH$ solvent mixtures (Figure 6).

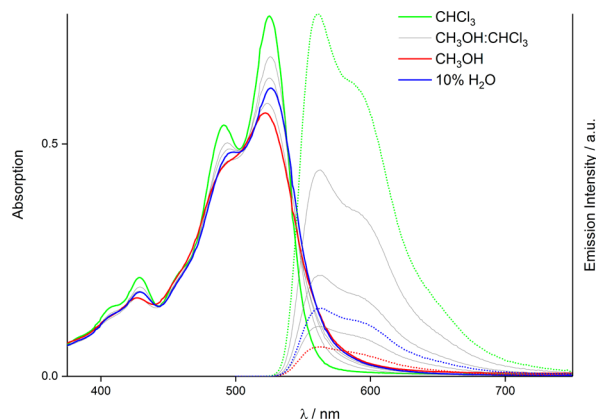


Figure 6. Electronic absorption (solid line) and fluorescence emission (dotted line) spectra of $3 \cdot (PF_6)_2$ measured in increasingly polar $CHCl_3:CH_3OH$ solvent mixtures and 10% H_2O (45:45:10 $CHCl_3:CH_3OH:H_2O$) (10^{-4} M, $\lambda_{ex} = 500$ nm).

The well resolved vibronic fine structure of the S_0-S_1 PDI absorption band persistent in all UV–vis spectra of $3 \cdot (PF_6)_2$, even at a relatively high concentration of 10^{-4} M, indicates that the PDI [3]catenane exists as a monomeric species in solution.^{54,56} This is to be expected because the highly twisted bay substituted tetrachloro PDI-containing molecules are known to exhibit some of the lowest self-aggregation constants of PDI-derivatives, even at up to mM concentrations.^{66,68,101}

Increasing the proportion of polar protic solvent (CH_3OH or H_2O) in the [3]catenane solution results in a significant reduction in intensity of the main PDI absorption band ($\lambda_{abs,max}$

≈ 525 nm) and the appearance of new absorption bands at longer wavelength ($\lambda_{abs} > 550$ nm). Based upon similar observations by Würthner et al. in the UV–vis spectra of charge-transfer complexes formed by PDI cyclophanes,^{102,103} the feature at $\lambda_{abs} > 550$ nm is attributed to charge-transfer bands arising from donor–acceptor aromatic stacking interactions between the electron-rich hydroquinone groups of the macrocycles and the electron-deficient tetrachloro PDI motif.¹⁰⁴ Furthermore, the formation of several isosbestic points indicate the establishment of a thermodynamic equilibrium between co-conformations as the peripheral macrocycles move from the triazolium to PDI stations. This is in line with the findings from the 1H NMR spectroscopic and MD studies.

Importantly, the solvent-induced changes seen in the UV–vis spectra of [3]catenane $3 \cdot (PF_6)_2$ are a direct consequence of circumrotatory macrocycle motion driven by intramolecular interactions with the PDI stations and not the formation of PDI aggregates by intermolecular aromatic stacking (see SI, section 5.2),^{57–59,105,106} because there is only a small solvent dependence to the electronic absorption spectrum of the PDI macrocycle $1 \cdot (BF_4)_2$ (Figure S21a). Further analysis of the vibronic progression of the S_0-S_1 PDI absorption band reveals a nearly constant A_{0-0}/A_{0-1} ratio of 1.44 for the macrocycle in each solvent, while the decrease of A_{0-0}/A_{0-1} from 1.43 to 1.22 for the [3]catenane upon changing from $CHCl_3$ to $MeOH$ is indicative of the emergence of aromatic stacking interactions involving PDI (Figures 6 and S21a).^{107,108} The absence of absorptions at $\lambda_{abs} > 550$ nm in the UV spectra results in the macrocycle $1 \cdot (BF_4)_2$ solution remaining orange under all solvent conditions (Figure S21b). Therefore, courtesy of its inherent circumrotational motion, the [3]catenane is able to distinguish between solvents and so can potentially be utilized as a novel molecular probe for colorimetric solvent sensing.

The solvent-induced co-conformational change exhibited by [3]catenane $3 \cdot (PF_6)_2$ was also investigated by fluorescence spectroscopy at the same concentration (Figure 6). As expected, the emergence of additional non-radiative decay channels such as charge-transfer interactions, as the peripheral macrocycles move to interact with the PDI stations of the central ring causes substantial quenching of the PDI fluorescence emission intensity, with this effect becoming more pronounced (up to 92%¹⁰⁹) in increasingly polar solvent media. Interestingly, a significant decrease in emission intensity (86%) is also observed for the free PDI macrocycle $1 \cdot (BF_4)_2$, which indicates that the solvent dependence of the decay pathway of the PDI excited state in the [3]catenane cannot be ascribed to only the dynamic behavior of the macrocycles (Figure S22). However, dilution of $1 \cdot (BF_4)_2$ and $3 \cdot (PF_6)_2$ to 10^{-7} M produced the same results (Figure S23), which, as well as the absence of red-shifted PDI excimer-type emission^{101,110,111} at high concentration, suggests that aggregate-induced quenching^{88,112} is not a significant mechanism in these systems. Instead, quenching may occur by a competitive charge-transfer process from neighboring electron-rich substituents to PDI.¹¹³

Optical Anion Sensing Studies. In similar fashion to the protic solvent stimulus, the addition of tetrabutylammonium (TBA) chloride to a solution of $3 \cdot (PF_6)_2$ in 3:1 $CHCl_3:CH_3OH$ caused a significant naked-eye detectable color change from red to orange (Figure 7). UV–visible anion titration experiments revealed this was concomitant with a hypsochromic shift of $\lambda_{abs,max}$ and a decrease in the intensity of the

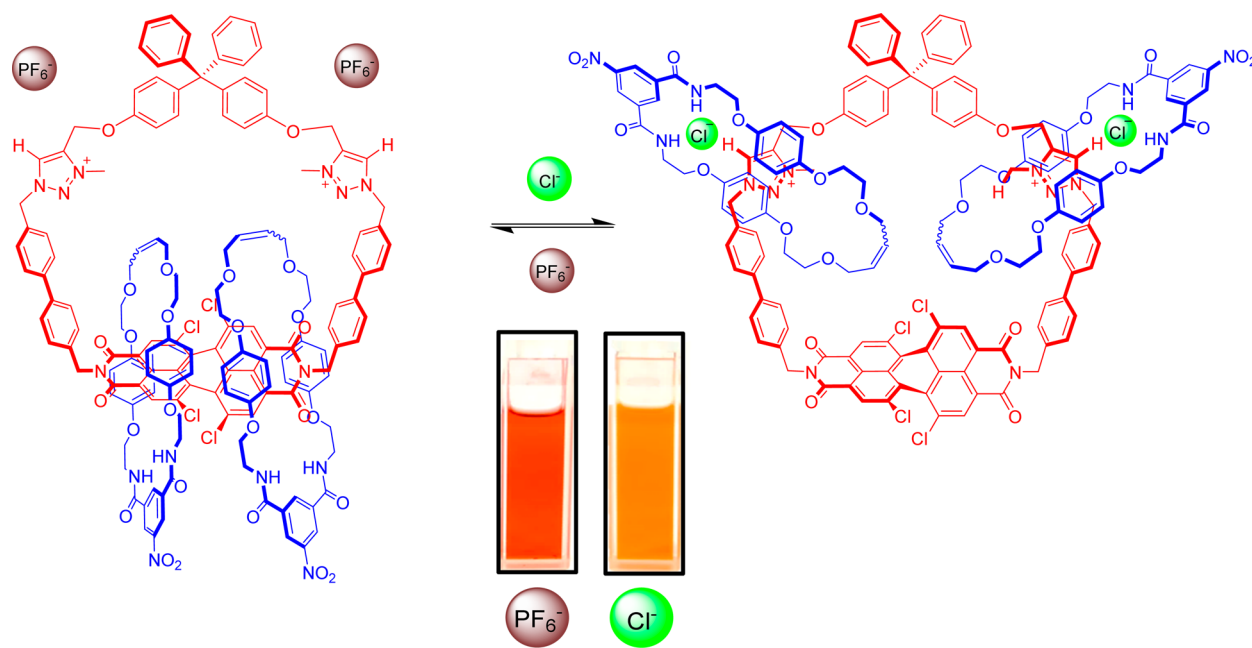


Figure 7. Anion-induced circumrotatory motion in the hetero[3]catenane and the colors associated with each anion.

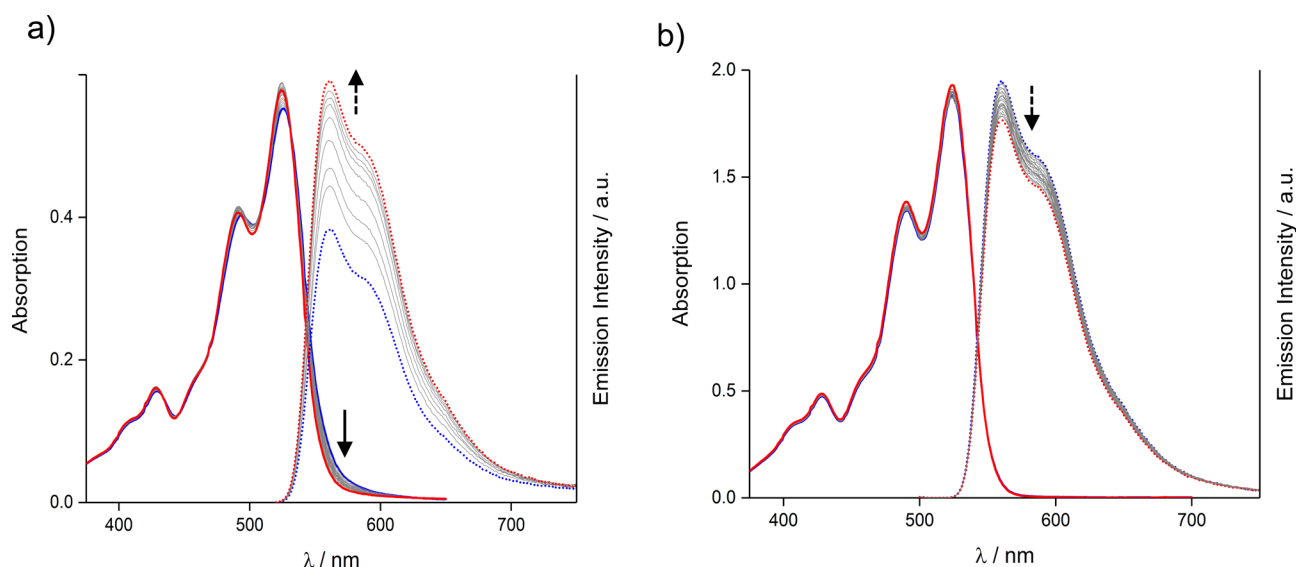


Figure 8. Electronic absorption (solid line) and fluorescence emission (dotted line) spectra of (a) [3]catenane $3 \cdot (\text{PF}_6)_2$ and (b) PDI macrocycle $1 \cdot (\text{BF}_4)_2$ upon the titration of 60 equiv of TBA-Cl (3:1 CHCl_3 : CH_3OH , 10^{-4} M for UV-vis and 10^{-7} M for fluorescence emission spectra, $\lambda_{\text{ex}} = 500$ nm, blue line = start point, red line = end point).

absorption bands at $\lambda_{\text{abs}} > 550$ nm (Figure 8a) resulting from the loss of intramolecular interactions between the PDI stations and the peripheral hydroquinone-containing macrocycles.

This halide anion-mediated dynamic behavior, characterized by ^1H NMR spectroscopy and MD studies, was also investigated by fluorescence spectroscopy¹¹⁴ with a notable increase in the PDI emission intensity (quantum yield enhancement factor of 57%¹⁰⁹) being observed upon addition of 60 equiv of chloride (Figure 8a). As expected from the ^1H NMR spectroscopic studies, the same turn-on fluorescent response was also produced in DMSO (Figure S24). Importantly, confirmation that the large-amplitude chloride anion-binding-induced circumrotatory molecular motion (Figure 7 and SI, section 5.2) is responsible for these changes was verified by no such optical responses being observed in the

absorption or emission spectra for the central PDI macrocycle $1 \cdot (\text{BF}_4)_2$ (Figure 8b) or indeed when the experiments were repeated with the [3]catenane $3 \cdot (\text{PF}_6)_2$ in neat CHCl_3 (Figure S25).

In addition to chloride, optical anion sensing was also observed upon the addition of other TBA oxoanion salts to a solution of $3 \cdot (\text{PF}_6)_2$ in 3:1 CHCl_3 : CH_3OH (Figure S26). The formation of several isosbestic points in the UV-vis titration spectra permitted quantitative analysis using Bindfit,¹¹⁵ which revealed 1:2 host:guest stoichiometric binding for all mono-anionic guests with a trend in binding strength that correlates with their basicity (Table 1 and SI, section 6).¹¹⁶

Besides the changes in the electronic absorption spectra, the exquisite sensing capabilities of [3]catenane $3 \cdot (\text{PF}_6)_2$ are also demonstrated in the significant turn-on fluorescence emission

Table 1. Anion Association Constants (M^{-1}) for [3]Catenane $3 \cdot (PF_6)_2$ Determined by UV–Vis Spectroscopy in 3:1 $CHCl_3:CH_3OH$ (298 K, $\lambda_{abs} = 540–590$ nm, 10^{-4} M)^a

	$\log(K_{11})$	$\log(K_{12})$
NO_3^-	3.77	3.17
Cl^-	4.19	2.20
$H_2PO_4^-$	>5	3.76
AcO^-	>5	4.26
SO_4^{2-}	3.88 ^b	–

^aAnions added as TBA salts. Errors <10%. ^bTitration performed in 45:45:10 $CHCl_3:CH_3OH:H_2O$, $\lambda_{abs} = 530–480$ nm.

response, which reports the recognition of anions at a low guest concentration (10^{-5} M) and in a competitive aqueous–organic solvent medium of 45:45:10 $CHCl_3:CH_3OH:H_2O$ (Figure S27 and Table S6).

CONCLUSIONS

A rare example of a dynamic hetero[3]catenane comprised of a large central four-station tetrachloro perylene diimide–bis-triazolium ring and two smaller peripheral isophthalamide-containing macrocycles was synthesized by anion templation and isolated as coordinating chloride and non-coordinating hexafluorophosphate anion salts.

NMR, UV–vis, and fluorescence emission spectroscopies and molecular dynamics simulations were employed to comprehensively study the interlocked structure's rotary dynamic behavior in a chloroform–methanol solvent mixture. These techniques demonstrated that with the hetero[3]-catenane $3 \cdot (PF_6)_2$, chloride anion-induced circumrotatory motion of the smaller macrocyclic rings from the core-substituted PDI motif to the two triazolium groups occurred upon anion recognition. Such unprecedented control over the rotary dynamics of an anion-binding [3]catenane enabled colorimetric and fluorescence anion sensing to be performed, notably in competitive protic organic and aqueous–organic solvent media. As mechanically interlocked molecular switches and machines begin to find applications in many areas of nanotechnology, this work serves to highlight the significant potential that molecular recognition stimulus-induced molecular motion has in the development of the next generation of sensory devices.

ASSOCIATED CONTENT

Supporting Information

The Supporting Information is available free of charge on the ACS Publications website at DOI: 10.1021/jacs.7b04295.

Further details of synthetic procedures, characterization, and spectroscopic and computational data, including Figures S1–S27 and Tables S1–S6 (PDF)
Movie S1 (ZIP)

AUTHOR INFORMATION

Corresponding Author

*paul.beer@chem.ox.ac.uk

ORCID

Igor Marques: 0000-0003-4971-9932

Paul D. Beer: 0000-0003-0810-9716

Notes

The authors declare no competing financial interest.

ACKNOWLEDGMENTS

The theoretical studies were supported by project P2020-PTDC/QEQ-SUP/4283/2014 as well as by CICECO–Aveiro Institute of Materials (UID/CTM/50011/2013) and iBiMED–Institute of Biomedicine (UID/BIM/04501/2013), financed by National Funds through the FCT/MEC and, when applicable, co-financed by FEDER through COMPETE, under the PT2020 Partnership Agreement. I.M. thanks the FCT for the Ph.D. scholarship SFRH/BD/87520/2012. T.A.B. would like to thank the EPSRC and Christ Church, University of Oxford, for funding.

REFERENCES

- (1) Anelli, P. L.; Spencer, N.; Stoddart, J. F. *J. Am. Chem. Soc.* **1991**, *113*, 5131.
- (2) Erbas-Cakmak, S.; Leigh, D. A.; McTernan, C. T.; Nussbaumer, A. L. *Chem. Rev.* **2015**, *115*, 10081.
- (3) Kay, E. R.; Leigh, D. A. *Angew. Chem., Int. Ed.* **2015**, *54*, 10080.
- (4) Van Noorden, R.; Castelvetti, D. *Nature* **2016**, *538*, 152.
- (5) Stoddart, J. F. *Acc. Chem. Res.* **2001**, *34*, 410.
- (6) Stoddart, J. F. *Chem. Soc. Rev.* **2009**, *38*, 1802.
- (7) Coskun, A.; Banaszak, M.; Astumian, R. D.; Stoddart, J. F.; Grzybowski, B. A. *Chem. Soc. Rev.* **2012**, *41*, 19.
- (8) Neal, E. A.; Goldup, S. M. *Chem. Commun.* **2014**, *50*, 5128.
- (9) McConnell, A. J.; Wood, C. S.; Neelakandan, P. P.; Nitschke, J. R. *Chem. Rev.* **2015**, *115*, 7729.
- (10) Zhu, K.; O'Keefe, C. A.; Vukotic, V. N.; Schurko, R. W.; Loeb, S. *J. Nat. Chem.* **2015**, *7*, 514.
- (11) Zhang, Z.-J.; Han, M.; Zhang, H.-Y.; Liu, Y. *Org. Lett.* **2013**, *15*, 1698.
- (12) Collin, J.-P.; Durola, F.; Heitz, V.; Reviriego, F.; Sauvage, J.-P.; Trolez, Y. *Angew. Chem., Int. Ed.* **2010**, *49*, 10172.
- (13) Collin, J.-P.; Durola, F.; Frey, J.; Heitz, V.; Reviriego, F.; Sauvage, J.-P.; Trolez, Y.; Rissanen, K. *J. Am. Chem. Soc.* **2010**, *132*, 6840.
- (14) Nagawa, Y.; Suga, J.; Hiratani, K.; Koyama, E.; Kanesato, M. *Chem. Commun.* **2005**, 749.
- (15) Barendt, T. A.; Docker, A.; Marques, I.; Félix, V.; Beer, P. D. *Angew. Chem., Int. Ed.* **2016**, *55*, 11069.
- (16) Frey, J.; Tock, C.; Collin, J.-P.; Heitz, V.; Sauvage, J.-P. *J. Am. Chem. Soc.* **2008**, *130*, 4592.
- (17) Marois, J.-S.; Cantin, K.; Desmarais, A.; Morin, J.-F. *Org. Lett.* **2008**, *10*, 33.
- (18) Balzani, V.; Clemente-León, M.; Credi, A.; Ferrer, B.; Venturi, M.; Flood, A. H.; Stoddart, J. F. *Proc. Natl. Acad. Sci. U. S. A.* **2006**, *103*, 1178.
- (19) Wang, Q.-C.; Qu, D.-H.; Ren, J.; Chen, K.; Tian, H. *Angew. Chem., Int. Ed.* **2004**, *43*, 2661.
- (20) Raiteri, P.; Bussi, G.; Cucinotta, C. S.; Credi, A.; Stoddart, J. F.; Parrinello, M. *Angew. Chem., Int. Ed.* **2008**, *47*, 3536.
- (21) Brouwer, A. M.; Frochot, C.; Gatti, F. G.; Leigh, D. A.; Mottier, L.; Paolucci, F.; Roffia, S.; Wurpel, G. W. H. *Science* **2001**, *291*, 2124.
- (22) Marlin, D. S.; González Cabrera, D.; Leigh, D. A.; Slawin, A. M. Z. *Angew. Chem., Int. Ed.* **2006**, *45*, 77.
- (23) Berná, J.; Alajarin, M.; Orenes, R.-A. *J. Am. Chem. Soc.* **2010**, *132*, 10741.
- (24) Zhang, Z.; Han, C.; Yu, G.; Huang, F. *Chem. Sci.* **2012**, *3*, 3026.
- (25) Gao, L.; Zhang, Z.; Zheng, B.; Huang, F. *Polym. Chem.* **2014**, *5*, 5734.
- (26) Kay, E. R.; Leigh, D. A.; Zerbetto, F. *Angew. Chem., Int. Ed.* **2007**, *46*, 72.
- (27) Amendola, V.; Fabbrizzi, L.; Mangano, C.; Pallavicini, P. *Acc. Chem. Res.* **2001**, *34*, 488.
- (28) Collin, J.-P.; Dietrich-Buchecker, C.; Gaviña, P.; Jimenez-Molero, M. C.; Sauvage, J.-P. *Acc. Chem. Res.* **2001**, *34*, 477.
- (29) Berná, J.; Franco-Pujante, C.; Alajarin, M. *Org. Biomol. Chem.* **2014**, *12*, 474.

- (30) Spence, G. T.; Pitak, M. B.; Beer, P. D. *Chem. - Eur. J.* **2012**, *18*, 7100.
- (31) Serpell, C. J.; Chall, R.; Thompson, A. L.; Beer, P. D. *Dalton Trans.* **2011**, *40*, 12052.
- (32) Dzyuba, E. V.; Kaufmann, L.; Löw, N. L.; Meyer, A. K.; Winkler, H. D. F.; Rissanen, K.; Schalley, C. A. *Org. Lett.* **2011**, *13*, 4838.
- (33) Gassensmith, J. J.; Matthys, S.; Lee, J.-J.; Wojcik, A.; Kamat, P. V.; Smith, B. D. *Chem. - Eur. J.* **2010**, *16*, 2916.
- (34) Zheng, H.; Zhou, W.; Lv, J.; Yin, X.; Li, Y.; Liu, H.; Li, Y. *Chem. - Eur. J.* **2009**, *15*, 13253.
- (35) Lin, T.-C.; Lai, C.-C.; Chiu, S.-H. *Org. Lett.* **2009**, *11*, 613.
- (36) Barrell, M. J.; Leigh, D. A.; Lusby, P. J.; Slawin, A. M. Z. *Angew. Chem., Int. Ed.* **2008**, *47*, 8036.
- (37) Keaveney, C. M.; Leigh, D. A. *Angew. Chem., Int. Ed.* **2004**, *43*, 1222.
- (38) Lin, C.-F.; Lai, C.-C.; Liu, Y.-H.; Peng, S.-M.; Chiu, S.-H. *Chem. - Eur. J.* **2007**, *13*, 4350.
- (39) Huang, Y.-L.; Hung, W.-C.; Lai, C.-C.; Liu, Y.-H.; Peng, S.-M.; Chiu, S.-H. *Angew. Chem., Int. Ed.* **2007**, *46*, 6629.
- (40) Liu, L.; Liu, Y.; Liu, P.; Wu, J.; Guan, Y.; Hu, X.; Lin, C.; Yang, Y.; Sun, X.; Ma, J.; Wang, L. *Chem. Sci.* **2013**, *4*, 1701.
- (41) Raju, M. V. R.; Lin, H.-C. *Org. Lett.* **2013**, *15*, 1274.
- (42) Zhang, H.; Hu, J.; Qu, D.-H. *Org. Lett.* **2012**, *14*, 2334.
- (43) Barendt, T. A.; Robinson, S. W.; Beer, P. D. *Chem. Sci.* **2016**, *7*, 5171.
- (44) Ng, K.-Y.; Felix, V.; Santos, S. M.; Rees, N. H.; Beer, P. D. *Chem. Commun.* **2008**, 1281.
- (45) Evans, N. H.; Serpell, C. J.; Beer, P. D. *Chem. - Eur. J.* **2011**, *17*, 7734.
- (46) Sessler, J. L.; Gale, P. A.; Cho, W.-S. In *Anion Receptor Chemistry*; RSC Publishing: Cambridge, UK, 2006.
- (47) Evans, N. H.; Beer, P. D. *Chem. Soc. Rev.* **2014**, *43*, 4658.
- (48) Evans, N. H.; Beer, P. D. *Angew. Chem., Int. Ed.* **2014**, *53*, 11716.
- (49) Gil-Ramírez, G.; Leigh, D. A.; Stephens, A. J. *Angew. Chem., Int. Ed.* **2015**, *54*, 6110.
- (50) Andrievsky, A.; Ahuis, F.; Sessler, J. L.; Vögtle, F.; Gudat, D.; Moini, M. J. *Am. Chem. Soc.* **1998**, *120*, 9712.
- (51) It is important to note that two distinct rotary motions are possible in a heterocatenane.⁵² The rotational motion of a smaller ring around a larger one is commonly referred to as “circumrotation”, while “pirouetting” denotes the simpler rotation of the smaller macrocycle on its own axis. Differentiation between these motions is made to allow comparisons with respective “shuttling” and “pirouetting” dynamics exhibited by rotaxanes.
- (52) Bruns, C. J.; Stoddart, J. F. In *The Nature of the Mechanical Bond*; John Wiley & Sons, Inc.; Hoboken, NJ, 2017.
- (53) In a previous attempt to produce anion-induced rotary motion in a [2]heterocatenane, acid/base control of phenoxide recognition was revealed to enforce an established co-conformation.⁴⁴
- (54) Würthner, F. *Chem. Commun.* **2004**, 1564.
- (55) Würthner, F.; Saha-Möller, C. R.; Fimmel, B.; Ogi, S.; Leowanawat, P.; Schmidt, D. *Chem. Rev.* **2016**, *116*, 962.
- (56) Huang, C.; Barlow, S.; Marder, S. R. *J. Org. Chem.* **2011**, *76*, 2386.
- (57) Chen, Z.; Fimmel, B.; Würthner, F. *Org. Biomol. Chem.* **2012**, *10*, 5845.
- (58) D'Anna, F.; Marullo, S.; Lazzara, G.; Vitale, P.; Noto, R. *Chem. - Eur. J.* **2015**, *21*, 14780.
- (59) Würthner, F.; Thalacker, C.; Diele, S.; Tschierske, C. *Chem. - Eur. J.* **2001**, *7*, 2245.
- (60) Görl, D.; Zhang, X.; Würthner, F. *Angew. Chem., Int. Ed.* **2012**, *51*, 6328.
- (61) Li, Y.; Li, H.; Li, Y.; Liu, H.; Wang, S.; He, X.; Wang, N.; Zhu, D. *Org. Lett.* **2005**, *7*, 4835.
- (62) Slater, B. J.; Davies, E. S.; Argent, S. P.; Nowell, H.; Lewis, W.; Blake, A. J.; Champness, N. R. *Chem. - Eur. J.* **2011**, *17*, 14746.
- (63) Wang, W.; Wang, L.; Palmer, B. J.; Exarhos, G. J.; Li, A. D. Q. *J. Am. Chem. Soc.* **2006**, *128*, 11150.
- (64) Boer, S. A.; Hawes, C. S.; Turner, D. R. *Chem. Commun.* **2014**, 50, 1125.
- (65) Baggerman, J.; Jagesar, D. C.; Vallée, R. A. L.; Hofkens, J.; De Schryver, F. C.; Schelhase, F.; Vögtle, F.; Brouwer, A. M. *Chem. - Eur. J.* **2007**, *13*, 1291.
- (66) Würthner, F. *Pure Appl. Chem.* **2006**, *78*, 2341.
- (67) Osswald, P.; Würthner, F. *J. Am. Chem. Soc.* **2007**, *129*, 14319.
- (68) Chen, Z.; Debije, M. G.; Debaerdemaeker, T.; Osswald, P.; Würthner, F. *ChemPhysChem* **2004**, *5*, 137.
- (69) Atropisomerism of the tetrachloro PDI motif translates into the observed diastereotopicity of H_{1/2} in the ¹H NMR spectrum of PDI macrocycle 1-(Cl)₂ (see SI). However, isolation of single chiral conformers (enantiomers) is not possible because they have been shown to slowly interconvert at room temperature.^{66,67,70}
- (70) Wang, W.; Shaller, A. D.; Li, A. D. Q. *J. Am. Chem. Soc.* **2008**, *130*, 8271.
- (71) The *trans* form of the alkene is expected to dominate in the vinyl-containing macrocycles,⁷² but the exact ratio of isomers could not be distinguished by low-temperature ¹H NMR spectroscopy (Figure S2a).
- (72) Mohr, B.; Sauvage, J. P.; Grubbs, R. H.; Weck, M. *Angew. Chem., Int. Ed. Engl.* **1997**, *36*, 1308.
- (73) This may also be caused by propagation of PDI atropisomerism to the peripheral macrocycles.
- (74) Cubberley, M. S.; Iverson, B. L. *J. Am. Chem. Soc.* **2001**, *123*, 7560.
- (75) Prentice, G. M.; Pascu, S. I.; Filip, S. V.; West, K. R.; Pantoş, G. D. *Chem. Commun.* **2015**, 51, 8265.
- (76) Ghosh, S.; Ramakrishnan, S. *Angew. Chem., Int. Ed.* **2004**, *43*, 3264.
- (77) Cockcroft, S. L.; Hunter, C. A. *Chem. Commun.* **2006**, 3806.
- (78) Martinez, C. R.; Iverson, B. L. *Chem. Sci.* **2012**, *3*, 2191.
- (79) Ikkanada, B. A.; Iverson, B. L. *Chem. Commun.* **2016**, 52, 7752.
- (80) Hunter, C. A.; Sanders, J. K. M. *J. Am. Chem. Soc.* **1990**, *112*, 5525.
- (81) Hunter, C. A. *Chem. Soc. Rev.* **1994**, *23*, 101.
- (82) Smithrud, D. B.; Diederich, F. *J. Am. Chem. Soc.* **1990**, *112*, 339.
- (83) Smithrud, D. B.; Wyman, T. B.; Diederich, F. *J. Am. Chem. Soc.* **1991**, *113*, 5420.
- (84) Diederich, F. *Angew. Chem., Int. Ed. Engl.* **1988**, *27*, 362.
- (85) Hwang, J.; Li, P.; Shimizu, K. D. *Org. Biomol. Chem.* **2017**, *15*, 1554.
- (86) Shao, C.; Grüne, M.; Stolte, M.; Würthner, F. *Chem. - Eur. J.* **2012**, *18*, 13665.
- (87) Chen, Z.; Stepanenko, V.; Dehm, V.; Prins, P.; Siebbeles, L. D. A.; Seibt, J.; Marquetand, P.; Engel, V.; Würthner, F. *Chem. - Eur. J.* **2007**, *13*, 436.
- (88) Decomposition and solvent-induced aggregation⁸⁴ were both ruled out as causes for this (see Figures S4–S6).
- (89) Wescott, L. D.; Mattern, D. L. *J. Org. Chem.* **2003**, *68*, 10058.
- (90) Langhals, H.; Demmig, S.; Potrawa, T. *J. Prakt. Chem.* **1991**, *333*, 733.
- (91) Langhals, H. *Heterocycles* **1995**, *40*, 477.
- (92) The NMR spectra of the bis-chloride salt of the [3]catenane were also complex, indicating some residual macrocycle interactions with the PDI stations under these solvent conditions (Figure S12). This complexity negated quantitative estimation of percentage occupancies of the respective stations from being determined.
- (93) Case, D. A.; Berryman, J. T.; Betz, R. M.; Cerutti, D. S.; Cheatham, T. E., III; Darden, T. A.; Duke, R. E.; Giese, T. J.; Gohlke, H.; Goetz, A. W.; Homeyer, N.; Izadi, S.; Janowski, P.; Kaus, J.; Kovalenko, A.; Lee, T. S.; LeGrand, S.; Li, P.; Luchko, T.; Luo, R.; Madej, B.; Merz, K. M.; Monard, G.; Needham, P.; Nguyen, H.; Nguyen, H. T.; Omelyan, I.; Onufriev, A.; Roe, D. R.; Roitberg, A.; Salomon-Ferrer, R.; Simmerling, C. L.; Smith, W.; Swails, J.; Walker, R. C.; Wang, J.; Wolf, R. M.; Wu, X.; York, D. M. and P. A. Kollman (2016), AMBER 2016, University of California: San Francisco.
- (94) Wang, J.; Wolf, R. M.; Caldwell, J. W.; Kollman, P. A.; Case, D. A. *J. Comput. Chem.* **2004**, *25*, 1157.

- (95) Wang, J.; Wolf, R. M.; Caldwell, J. W.; Kollman, P. A.; Case, D. A. *J. Comput. Chem.* **2005**, *26*, 114.
- (96) Bayly, C. I.; Cieplak, P.; Cornell, W.; Kollman, P. A. *J. Phys. Chem.* **1993**, *97*, 10269.
- (97) Kilah, N. L.; Wise, M. D.; Beer, P. D. *Cryst. Growth Des.* **2011**, *11*, 4565.
- (98) Salomon-Ferrer, R.; Götz, A. W.; Poole, D.; Le Grand, S.; Walker, R. C. *J. Chem. Theory Comput.* **2013**, *9*, 3878.
- (99) The MD simulations of $3A^-(Cl)_2$ revealed that the hydrogen bonds between the chloride anion and both peripheral macrocycles have shorter $N\cdots Cl^-$ distances and more-linear $N-H\cdots Cl^-$ angles, with smaller standard deviations in pure chloroform (Table S2) than in the solvent mixture (Table S1). In other words, this comparison indicates that the two isophthalamide clefts are more tightly bonded to the chloride anions in the less polar solvent medium.
- (100) C_{HYD} corresponds to the center of mass of the carbon atoms from the hydroquinone rings of the peripheral macrocycles, while C_{PDI} is the center of mass defined by the non-hydrogen atom of the three six-membered rings (benzo[de]isoquinoline moiety) on each side of the PDI.
- (101) Chen, Z.; Baumeister, U.; Tschierske, C.; Würthner, F. *Chem. - Eur. J.* **2007**, *13*, 450.
- (102) Spenst, P.; Würthner, F. *Angew. Chem., Int. Ed.* **2015**, *54*, 10165.
- (103) Spenst, P.; Sieblist, A.; Würthner, F. *Chem. - Eur. J.* **2017**, *23*, 1667.
- (104) In addition it should be noted that Vögtle⁶⁵ has attributed a red shift in the PDI absorption band to the participation of the imide carbonyl groups in hydrogen-bonding interactions, which, as demonstrated in the MD studies, is also a possibility in the [3] catenane.
- (105) Zhang, X.; Chen, Z.; Würthner, F. *J. Am. Chem. Soc.* **2007**, *129*, 4886.
- (106) Wang, W.; Wan, W.; Zhou, H.-H.; Niu, S.; Li, A. D. Q. *J. Am. Chem. Soc.* **2003**, *125*, 5248.
- (107) Seibt, J.; Marquetand, P.; Engel, V.; Chen, Z.; Dehm, V.; Würthner, F. *Chem. Phys.* **2006**, *328*, 354.
- (108) Spenst, P.; Young, R. M.; Phelan, B. T.; Keller, M.; Dostál, J.; Brixner, T.; Wasielewski, M. R.; Würthner, F. *J. Am. Chem. Soc.* **2017**, *139*, 2014.
- (109) Calculated by integration of peak intensities between $\lambda_{em} = 525$ and 700 nm.
- (110) Ahrens, M. J.; Sinks, L. E.; Rybtchinski, B.; Liu, W.; Jones, B. A.; Giaimo, J. M.; Gusev, A. V.; Goshe, A. J.; Tiede, D. M.; Wasielewski, M. R. *J. Am. Chem. Soc.* **2004**, *126*, 8284.
- (111) Würthner, F.; Chen, Z.; Dehm, V.; Stepanenko, V. *Chem. Commun.* **2006**, 1188.
- (112) Ma, X.; Sun, R.; Cheng, J.; Liu, J.; Gou, F.; Xiang, H.; Zhou, X. *J. Chem. Educ.* **2016**, *93*, 345.
- (113) Osswald, P.; Würthner, F. *Chem. - Eur. J.* **2007**, *13*, 7395.
- (114) In order to definitively ensure the existence of monomeric species in solution, these experiments were performed at a low concentration of 10^{-7} M.
- (115) www.supramolecular.org
- (116) For sulfate, $\log(K_{1/12}) > 5$, and so an anion association constant was obtained in 45:45:10 $CHCl_3$: CH_3OH : H_2O . Titration with nitrate, hydrogen phosphate, or acetate in this solvent produced UV-vis spectral changes that could not be reliably fitted to a stoichiometric host:guest model. This implies complex binding equilibria with these species.